

# Fluid inertial torque is an effective gyrotactic mechanism for settling elongated micro-swimmers

Jingran Qiu,<sup>1</sup> Zhiwen Cui,<sup>1</sup> Eric Climent,<sup>2</sup> and Lihao Zhao<sup>1,\*</sup>

<sup>1</sup> *AML, Department of Engineering Mechanics, Tsinghua University, 100084 Beijing, China*

<sup>2</sup> *Institut de Mécanique des Fluides de Toulouse (IMFT), UMR5502 Université de Toulouse, CNRS. Allée du Prof. Camille Soula – 31400 Toulouse, France*

(Dated: December 22, 2024)

Marine plankton are usually modeled as settling elongated micro-swimmers. For the first time, we consider the torque induced by fluid inertia on such swimmers, and we discover that they spontaneously swim in the direction opposite to gravity. Using direct numerical simulations, we examine the statistics of the orientation and spatial clustering of such swimmers in both quiescent fluid and turbulent flows. When the swimming velocity is greater than the settling speed, swimmers preferentially align in the upward direction due to fluid inertial torque. This torque also induces spatial clustering and preferential sampling of upwelling or downwelling flow regions depending on the swimming and settling speeds. Our findings suggest that the fluid inertial torque is a new mechanism of gyrotaxis that stabilizes the upward orientation of micro-swimmers such as plankton.

**Keywords:** swimmer, turbulence, gravitaxis, fluid inertia

## INTRODUCTION

Plankton play an important role in marine ecosystem. For instance, plankton produce oxygen by photosynthesis, and transfer energy to zooplankton and other marine predators in the food web. Many motile plankton migrate vertically to pursue nutrients or to avoid predation [1–3]. The vertical migration is driven by gravity and other physical and chemical stimuli. The responses to these stimuli are known as gyrotaxis [4], phototaxis [5], and chemotaxis [6], etc. To understand the vertical migration for different species, one needs to understand the role of each taxis. In the present study, we focus on gyrotaxis, which produces a stabilizing torque due to gravity that reorients a micro-swimmer in the upward direction [4]. Gyrotaxis is found to affect the behavior of plankton without the presence of other stimuli, causing preferential swimming direction [7, 8] and spatial clustering [9–11].

Earlier studies proposed two mechanisms for the gyrotactic stability: the bottom heaviness [7] and fore-aft shape asymmetry [12, 13]. Both mechanisms produce a reorientation torque by changing the positions of centers of gravity force, hydrodynamic force and buoyancy. Based on these two regular mechanisms, gyrotactic swimmers are widely studied by modeling them as point-wise motile particles that swim relative to the fluid under gravitational torques [8–11, 14–17]. In particular, this idealized model neglects the effect of fluid inertia. However, recent studies indicated that the orientation of a spheroidal particle is affected by a fluid inertial torque when there is a velocity difference between the particle and the local fluid [18–20]. For instance, spheroidal particles with particle Reynolds number  $Re_p \ll 1$  settle with broad side down in turbulence under the influence of fluid inertial torque [18, 19], showing a different picture from the case without considering fluid inertia, in which particles settle with narrow side down [21, 22].

Motile plankton move relative to the local fluid due to their motility and gravitational settling. It is natural to ask whether and how the fluid inertial torque affects the behavior of micro-swimmers such as plankton. In this letter, we investigate the effect of fluid inertial torque on settling micro-swimmers in quiescent fluid and turbulent flows. Interestingly, without any regular mechanism of gyrotaxis, elongated settling micro-swimmers still reorient themselves in upward direction under the influence of fluid inertial torque. Statistical results of orientation and clustering of swimmers demonstrate that fluid inertial torque is a new mechanism of gyrotaxis, which is different from the two regular mechanisms of bottom-heaviness and fore-aft shape asymmetry.

## FLUID INERTIAL TORQUE ON MICRO-SWIMMERS

Plankton are usually modeled as point-wise spheroidal swimmers [8–10, 14, 15]. Fluid inertial force and torque on a spheroid originate from the leading-order effects of fluid inertia when the spheroid moves relative to the fluid

---

\* zhaolihao@mail.tsinghua.edu.cn

[20, 23]. The Reynolds number of a planktonic swimmer  $Re_p = |\mathbf{u} - \mathbf{v}_p| L / \gamma$  is usually much smaller than unity. Here,  $\mathbf{v}_p$  and  $\mathbf{u}$  are the velocities of the swimmer and local fluid, respectively,  $L$  is the swimmer length scale, and  $\gamma$  is the kinematic viscosity of fluid. In this regime, the fluid inertial force is negligible because its magnitude is of the order of  $Re_p$  smaller than the magnitude of Stokes drag [18, 23]. However, the fluid inertial torque can be significant compared to the Jeffery torque [24]. For instance, the ratio between the magnitudes of inertial torque and Jeffery torque in turbulence is proportional to  $|\mathbf{u} - \mathbf{v}_p| / u_\eta$  [18], where  $u_\eta$  is the Kolmogorov velocity scale. Hence, the fluid inertial torque is not necessarily negligible when  $Re_p \ll 1$ , especially when a swimmer moves relative to the fluid at a significant speed. A detailed dimensional analysis is provided in Supplemental Materials [25].

A micro-swimmer usually satisfies the overdamped limit, which means that the response time of the swimmer's motion is much shorter than the characteristic timescale of fluid motion [19]. Following Ref. [19], we build the model of a settling micro-swimmer (Figure 1) with the influence of fluid inertial torque (see Supplemental Materials [25]). In this model, the motion of a swimmer is governed by the following equations:

$$\dot{\mathbf{n}} = \boldsymbol{\omega}_p \times \mathbf{n}, \quad (1)$$

$$\mathbf{v}_p = \mathbf{u} + v_{\text{swim}} \mathbf{n} + \mathbf{v}_{\text{settle}}. \quad (2)$$

Here,  $\boldsymbol{\omega}_p$  is the swimmer angular velocity, and  $\mathbf{n}$  is the unit vector along its symmetry axis. The swimmer is assumed to swim at a constant speed in the direction of  $\mathbf{n}$ , and it is advected by the local fluid with velocity  $\mathbf{u}$ . Settling due to gravity is taken into account by adding a settling speed  $\mathbf{v}_{\text{settle}}$ . In the overdamped limit, a swimmer settling in a fluid flow satisfies the Stokesian flow assumption, and the settling speed is expressed as [25, 26]:

$$\mathbf{v}_{\text{settle}} = -v_1 \mathbf{e}_y - (v_3 - v_1) (\mathbf{e}_y \cdot \mathbf{n}) \mathbf{n}, \quad (3)$$

where  $v_1$  and  $v_3$  are the Stokesian terminal velocities of a spheroid in a quiescent fluid with its symmetry axis aligned orthogonal to and parallel to the gravity direction, respectively. We specify the direction of  $y$ -axis  $\mathbf{e}_y$  as the direction opposite to gravity, i.e.  $\mathbf{e}_y = -\mathbf{g} / |\mathbf{g}|$ .

The swimmer's angular velocity is expressed as [19, 25]:

$$\begin{aligned} \boldsymbol{\omega}_p = & \frac{1}{2} \boldsymbol{\omega} + \frac{\lambda^2 - 1}{\lambda^2 + 1} (\mathbf{n} \times \mathbb{S} \cdot \mathbf{n}) \\ & + \frac{M}{\gamma} [v_{\text{swim}} v_1 (\mathbf{e}_y \times \mathbf{n}) - v_1 v_3 (\mathbf{e}_y \cdot \mathbf{n}) (\mathbf{e}_y \times \mathbf{n})], \end{aligned} \quad (4)$$

where the first two terms on the right-hand-side originate from the Jeffery equations [24], and represent the contributions of local fluid vorticity  $\boldsymbol{\omega}$  and strain rate  $\mathbb{S}$ , respectively. The aspect ratio  $\lambda$  is defined as the length ratio between the major and minor axes of the spheroidal swimmer, with  $\lambda = 1$  for spheres and  $\lambda > 1$  for elongated spheroids. The third term on the right-hand-side of Eq. (4) is the contribution of fluid inertial torque, where the shape factor  $M$  only depends on  $\lambda$ , ranging from  $M = 0$  for  $\lambda = 1$ , to  $M \approx -0.1$  for  $\lambda = 2 \sim 8$  (see Supplemental Materials [25]).

The contribution of fluid inertial torque consists of two parts. The *swimming-settling term*  $M v_{\text{swim}} v_1 (\mathbf{e}_y \times \mathbf{n}) / \gamma$  denotes the coupling effect of swimming and settling, and the *settling term*  $-M v_1 v_3 (\mathbf{e}_y \cdot \mathbf{n}) (\mathbf{e}_y \times \mathbf{n}) / \gamma$  is only ascribed to settling effect. These two terms have a similar form as the angular velocity caused by the regular gyrotaxis torque,  $-(\mathbf{e}_y \times \mathbf{n}) / (2B)$ , where the reorientation time  $B$  represents how fast the orientation  $\mathbf{n}$  of a swimmer aligns to the upward direction  $\mathbf{e}_y$  [27]. In our case, the swimming-settling term results in an effective reorientation time of  $\gamma / (2|M| v_{\text{swim}} v_1)$ , whereas the settling term reduces the reorientation time by making a negative, orientation-dependent contribution  $-\gamma / (2|M| v_1 v_3 \mathbf{e}_y \cdot \mathbf{n})$ . Swimmers are expected to orient upward when the swimming-settling term dominates (e.g.  $v_{\text{swim}} \gg v_3$ ), and to align horizontally when the settling term is dominant (e.g.  $v_{\text{swim}} \ll v_3$ ). However, the stable orientation needs further analysis when  $v_{\text{swim}}$  and  $v_3$  are of the same order of magnitude.

## SETTLING SWIMMERS IN A QUIESCENT FLUID

To understand how fluid inertial torque affects the orientation of swimmers, we first analyze angular dynamics in a quiescent fluid. Using Eq. (4), the rotation of a swimmer is described as:

$$\frac{d\alpha}{dt} = \frac{M}{\gamma} (v_{\text{swim}} v_1 \sin \alpha - v_1 v_3 \cos \alpha \sin \alpha). \quad (5)$$

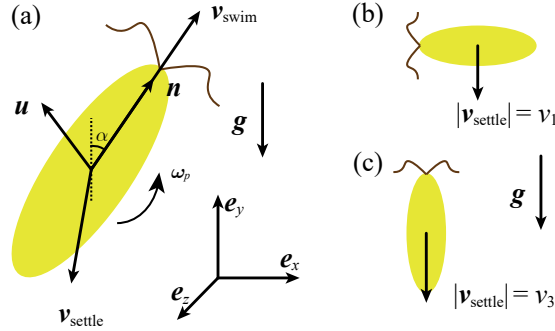


FIG. 1. (a) A sketch of a settling elongated swimmer.  $e_x$ ,  $e_y$ , and  $e_z$  are the base vectors of the global frame of reference. (b) A swimmer settling with the symmetry axis perpendicular to gravity. (c) A swimmer settling with its symmetry axis parallel to the direction of gravity.

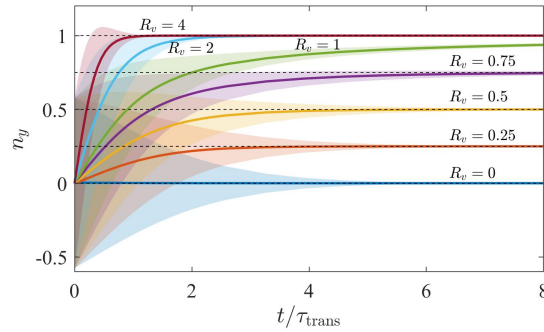


FIG. 2. Evolution of the orientation of swimmers  $n_y$  over dimensionless time  $t/\tau_{\text{trans}}$  in a quiescent fluid, where  $\tau_{\text{trans}} = \gamma/|M| v_1 v_3$  is a time scale for the transient regime according to Eq. (7). Solid lines represent the mean value of  $n_y$ , and the colored areas represent the ranges of mean  $\pm$  standard deviation. Horizontal dashed lines stand for the theoretical equilibrium orientation. The aspect ratio of swimmers is  $\lambda = 8$  for all cases here.

Here,  $\alpha$  is the angle of  $\mathbf{n}$  relative to  $e_y$  [Figure 1(a)], and thus  $n_y \equiv \mathbf{n} \cdot \mathbf{e}_y = \cos \alpha$ . From Eq. (5), a swimmer has three equilibrium orientations:

$$\alpha_0^{(1)} = 0, \quad \alpha_0^{(2)} = \arccos \frac{v_{\text{swim}}}{v_3}, \quad \text{and} \quad \alpha_0^{(3)} = \pi, \quad (6)$$

which correspond to (1) swimming upward against gravity, (2) swimming with a fixed angle relative to gravity direction, and (3) swimming downward along the gravity direction, respectively. Derived from Eq. (5), the first order linear equation of a small perturbation around the equilibrium orientations,  $\delta_\alpha$ , reads:

$$\frac{d\delta_\alpha}{dt} = \frac{Mv_1v_3}{\gamma} (R_v \cos \alpha_0 - \cos 2\alpha_0) \delta_\alpha, \quad (7)$$

where  $R_v = v_{\text{swim}}/v_3$ . With  $M < 0$ ,  $\alpha_0^{(3)}$  is always unstable, but the stability of  $\alpha_0^{(1)}$  and  $\alpha_0^{(2)}$  depends on  $R_v$ .

In general, a swimmer has only one stable orientation  $n_y = \min(1, R_v)$ . When  $R_v \leq 1$ , the swimming-settling term does not overcome the settling term, so the swimmer reaches an intermediate orientation where the two terms are balanced. When  $R_v > 1$ , the swimming-settling term overcomes the settling term for any orientation, so the swimmer rotates to swim upward. In such case, fluid inertial torque produces an effective gyrotaxis for the settling swimmer. Simulations in a quiescent fluid are performed to verify the aforementioned theoretical analysis. Figure 2 shows that swimmers with random initial orientation gradually approach the theoretical equilibrium orientation after a transient time. Mean orientation of swimmers converges in a short time when  $R_v > 1$ , but takes a longer transient time to converge when  $R_v < 1$ . The transient time is the longest in the critical case of  $R_v = 1$  (green line), and the swimming-settling term and settling term are almost balanced at  $n_y \approx 1$ , resulting in a small angular velocity.

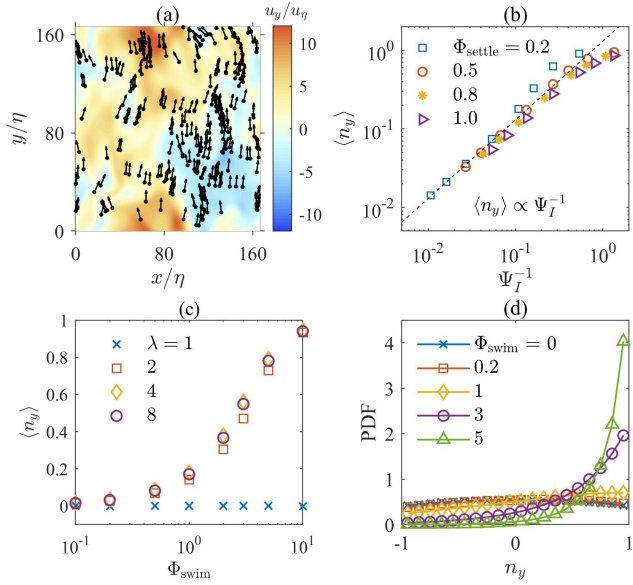


FIG. 3. (a) Instantaneous spatial distribution of swimmers in HIT. Black dots and tiny arrows stand for the position and swimming direction of each swimmer, respectively. Colors represent the vertical fluid velocity  $u_y$ . Quantities are normalized by Kolmogorov velocity and length scale,  $u_\eta$  and  $\eta$ , respectively. Parameters of swimmers are  $\Phi_{\text{settle}} = 0.5$ ,  $\Phi_{\text{swim}} = 10$ , and  $\lambda = 2$ , corresponding to  $\Psi_I = 0.99$ . (b) Mean orientation  $\langle n_y \rangle$  versus  $\Psi_I^{-1}$  with  $\lambda = 8$ . The slope of the dashed line represent the relationship of  $\langle n_y \rangle \propto \Psi_I^{-1}$ . (c)  $\langle n_y \rangle$  of swimmers with  $\Phi_{\text{settle}} = 0.5$  in HIT. (d) Probability distribution functions (PDFs) of  $n_y$  of swimmers in HIT with  $\lambda = 8$  and  $\Phi_{\text{settle}} = 0.5$ .

### ORIENTATION OF SWIMMERS IN TURBULENCE

In the ocean or estuaries, the behavior of planktonic micro-swimmers is usually influenced by a turbulent environment. Turbulence disturbs the orientation, and induces spatial clustering of swimmers [8–11]. Here, we investigate the influence of fluid inertial torque on settling swimmers in a homogeneous isotropic turbulence (HIT).

We use Eulerian-Lagrangian direct numerical simulations to obtain the trajectories of swimmers in a forced HIT with a Taylor Reynolds number  $\text{Re}_\lambda = u_{\text{rms}}^2 \sqrt{15}/(\gamma\epsilon) = 60$ , where  $u_{\text{rms}}$  and  $\epsilon$  are the root-mean square velocity and dissipation rate, respectively. The incompressible Navier-Stokes equations are solved by a pseudo-spectral method with  $96^3$  grid points to ensure the accuracy of resolution at small scales. To quantify the swimming and settling speeds in turbulence, we define two dimensionless parameters using Kolmogorov scales:  $\Phi_{\text{swim}} = v_{\text{swim}}/u_\eta$  and  $\Phi_{\text{settle}} = (2v_1 + v_3)/3u_\eta$ . We investigate swimmers within a parameter space of  $0 \leq \Phi_{\text{swim}} \leq 10$ ,  $0 \leq \Phi_{\text{settle}} \leq 1$ , and  $1 \leq \lambda \leq 8$ , corresponding to the typical values for oceanic plankton [14, 16, 28–30]. Statistics of each parameter configuration are obtained by averaging over 40 uncorrelated time samples of 120,000 trajectories. Details of numerical methods are provided in Supplemental Materials [25].

Figure 3(a) shows that elongated swimmers preferentially swim in upward direction fluid due to inertial torque. The swimming-settling term in Eq. (4), which provides effective gyrotaxis, is responsible for the upward orientation. Although the settling term weakens the effective gyrotaxis, it is negligible if  $\Phi_{\text{swim}} \gg \Phi_{\text{settle}}$ , or if swimmers do not preferentially align with upward direction ( $\langle n_y \rangle \approx 0$ , where  $\langle \cdot \rangle$  denotes the ensemble average). For the current parameters, either of the two situations happens. Therefore, we quantify the effective reorientation time scale by the swimming-settling term in Eq. (4) (see Supplemental Materials [25] for details), and define a dimensionless parameter

$$\Psi_I = (2|M|\Phi_{\text{swim}}\Phi_{\text{settle}})^{-1}. \quad (8)$$

Similar to the widely-used gyrotactic parameter  $\Psi = Bu_\eta/\eta$  [9–11], a smaller  $\Psi_I$  means a shorter reorientation time, and swimmers reorient to upward direction faster. Figure 3(b) shows that  $\langle n_y \rangle$  is approximately proportional to  $\Psi_I^{-1}$ , suggesting a strong correlation between the orientation of swimmers and  $\Psi_I$ .

Fluid inertial torque depends on  $\lambda$  through the shape factor  $M$ . As shown in Figure 3(c), spherical swimmers ( $\lambda = 1$ ) do not align with gravity, indicated by  $\langle n_y \rangle = 0$ . This is because fluid inertial torque vanishes as  $M = 0$  for  $\lambda = 1$ , and the isotropic fluid vorticity randomizes the orientation. However, when  $\lambda > 1$ , swimmers preferentially align in the upward direction, and  $\langle n_y \rangle$  is large when  $\lambda = 4$  and  $8$ , in which case  $|M|$  almost reaches the maximum and

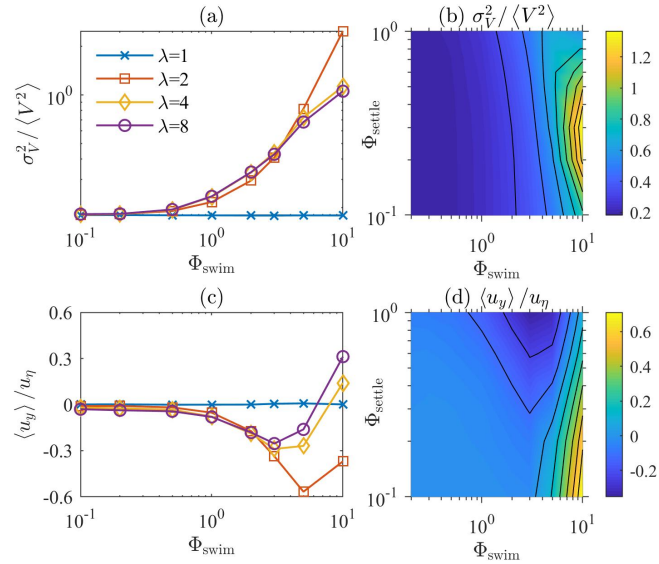


FIG. 4. Statistics of Voronoi volumes and preferential sampling of swimmers in turbulence. (a) Variance of Voronoi volumes  $\sigma_V^2$  of swimmers with  $\Phi_{\text{settle}} = 0.5$ , normalized by the mean square of Voronoi volumes  $\langle V^2 \rangle$ . (b) Normalized variance of Voronoi volumes of swimmers with  $\lambda = 8$ . (c) Mean vertical fluid velocity at swimmers' positions,  $\langle u_y \rangle$ , normalized by  $u_\eta$ .  $\Phi_{\text{settle}} = 0.5$ . (d) Mean vertical fluid velocity at swimmers' positions with  $\lambda = 8$ .

leads to a minimal  $\Psi_I$ . For elongated swimmers,  $\langle n_y \rangle$  monotonously increases with  $\Phi_{\text{swim}}$ , as the swimming-settling term in Eq. (4) dominates and acts as gyrotaxis with small  $\Psi_I$ . This is confirmed by the peaks at  $n_y = 1$  of orientation distribution in Figure 3(d). For swimmers with  $\Phi_{\text{swim}} = 0$ , earlier studies [18, 19, 31] reported that settling spheroids align perpendicular to gravity due to the settling term in Eq. (4). But this tendency is weak in our results, because the settling term is small for swimmers with  $\Phi_{\text{settle}} = 0.5$  that we only observe a slight peak at  $n_y = 0$  in Figure 3(d).

## I. CLUSTERING AND PREFERENTIAL SAMPLING OF SWIMMERS IN TURBULENCE

Another important effect of turbulence is that the flow structures allow gyrotactic swimmers to form spatial clusters and preferentially sample regions with downwelling or upwelling fluid velocity. As documented in earlier studies [8–11], these phenomena depend on the swimming speed, reorientation time, and the shape of swimmers. In our case, fluid inertial torque provides an effective reorientation time quantified by  $\Psi_I$ , so swimmers form clusters and preferentially sample specific flow regions as regular gyrotactic swimmers do. However, the trend over parameters may be different as  $\Psi_I$  depends on  $\Phi_{\text{swim}}$ ,  $\Phi_{\text{settle}}$  and  $\lambda$ . Here, we compare our results with earlier findings and discuss how these parameters affect the clustering and sampling of swimmers under the influence of fluid inertial torque.

We quantify the clustering of swimmers by three-dimensional Voronoi tessellations of the computational domain based on swimmers' positions [32]. A large variance of Voronoi volumes indicates strong clustering of swimmers. Figure 4(a) shows that spherical swimmers are always randomly distributed as fluid inertial torque is zero. Swimmers with  $\Phi_{\text{swim}} < 3$  (large  $\Psi_I$ ) form the strongest clusters when  $\lambda = 8$ . Conversely, when  $\Phi_{\text{swim}} > 3$  (small  $\Psi_I$ ), less elongated swimmers ( $\lambda = 2$ ) cluster the most. Our results are consistent with the observation on regular gyrotactic swimmers whose reorientation time is quantified by  $\Psi$  in Ref. [11]: with large  $\Psi$ , elongated swimmers are more clustered than spherical swimmers, but the opposite is true when  $\Psi$  is small. Figure 4(b) shows the intensity of clustering as a function of  $\Phi_{\text{swim}}$  and  $\Phi_{\text{settle}}$  for elongated swimmers. A peak is observed at large  $\Phi_{\text{swim}}$  and moderate  $\Phi_{\text{settle}}$ , which corresponds to  $\Psi_I \approx 1$  (see Fig. S2(b) in Supplemental Materials [25]). The location of this peak is consistent with earlier observation [8, 9] that maximal clustering occurs when gyrotactic swimmers swim fast and have  $\Psi \approx 1$ .

Gyrotactic swimmers preferentially sample the regions with upward or downward fluid velocity when the gravitational torque breaks the up-down symmetry [9–11]. Quantitative theoretical prediction [10] may fail in our case because the settling velocity interferes with the selection of sampling regions [33]. Nevertheless, our results in Figure 4(c) are qualitatively consistent with the tendency observed in Refs. [10, 11] that swimmers mostly sample downwelling regions ( $\langle u_y \rangle < 0$ ), but they also sample upwelling regions ( $\langle u_y \rangle > 0$ ) if  $\lambda$  is large and  $\Phi_{\text{swim}}$  exceeds a critical value. Figure 4(d) shows  $\langle u_y \rangle$  for swimmers with  $\lambda = 8$  over the parameter space of  $\Phi_{\text{swim}}$  and  $\Phi_{\text{settle}}$ . In most of the cases,

swimmers sample downwelling regions with  $\langle u_y \rangle < 0$ . When  $\Phi_{\text{settle}}$  approaches unity, which means a small  $\Psi_I$ , a significant sampling of downwelling regions is observed at  $\Phi_{\text{swim}} \approx 3$ . However, when  $\Phi_{\text{settle}}$  decreases ( $\Psi_I$  increases), it becomes easier for swimmers to reach the critical  $\Phi_{\text{swim}}$  and sample upwelling regions with  $\langle u_y \rangle > 0$ . Our results are consistent with earlier observations [11] that swimmers with small  $\Psi$  sample downwelling regions significantly when  $\Phi_{\text{swim}}$  is smaller than the aforementioned critical value, and that this critical  $\Phi_{\text{swim}}$  decreases as  $\Psi$  becomes larger. Our results suggest that swimmers with large  $\Phi_{\text{swim}}$  and small  $\Phi_{\text{settle}}$  may enhance the sampling of upwelling regions and benefit the upward migration for micro-swimmers.

## CONCLUSIONS

The present study discusses the significance of fluid inertial torque on settling micro-swimmers. The effect of fluid inertial torque in Eq. (4) shares a similar mathematical form with regular gyrotaxis mechanisms caused by bottom-heaviness or fore-aft asymmetry, providing a stabilizing torque that depends on the swimming and settling speeds and the shape of swimmers. Under the effect of fluid inertial torque, elongated settling swimmers tend to rotate and swim in the upward direction in both quiescent fluid and turbulent flows. Therefore, we conclude that fluid inertial torque is an effective mechanism of gyrotaxis for the settling swimmers. Using a dimensionless parameter  $\Psi_I$ , we show that orientation and clustering of swimmers in turbulence are strongly influenced by fluid inertial torque alone.

Fluid inertial torque may have a potential impact on the gyrotaxis for elongated planktonic swimmers, especially for those forming long chains and thus having large swimming and settling speeds [28, 34]. Moreover, unlike the two regular gyrotaxis mechanisms which contribute to the rotation dynamics passively, the fluid inertial torque can be tuned by the swimming speed. This feature provides a possible strategy for micro-swimmers to actively control the gyrotactic reorientation time by adjusting swimming velocity.

In previous studies concerning micro-swimmers in turbulence, the gravitational settling effect is often neglected [8–11, 14–17]. However, our results demonstrate that the settling effect not only affects the translation of a swimmer, but also contributes to its rotation through fluid inertial torque. In our case, neglecting settling leads to an underestimation of gyrotaxis because fluid inertial torque vanishes without settling effect. Therefore, the settling of plankton or other motile swimmers may not be simply neglected.

## ACKNOWLEDGMENTS

This work was supported by the National Natural Science Foundation of China (Grant No. 11911530141 and 91752205). JQ and LZ acknowledge the support from the Institute for Guo Qiang of Tsinghua University (Grant No. 2019GQQ1012).

---

[1] T. J. Smayda, *Limnology and Oceanography* **42**, 1137 (1997).

[2] G. C. Hays, *Migrations and dispersal of marine organisms*, 163 (2003).

[3] S. M. Bollens and B. Frost, *Journal of Plankton Research* **11**, 1047 (1989).

[4] O. Pundyak, *Oceanologia* **59**, 108 (2017).

[5] B. Eggersdorfer and D.-P. Häder, *FEMS Microbiology Letters* **85**, 319 (1991).

[6] R. Stocker, J. R. Seymour, A. Samadani, D. E. Hunt, and M. F. Polz, *Proceedings of the National Academy of Sciences* **105**, 4209 (2008).

[7] J. O. Kessler, *Journal of Fluid Mechanics* **173**, 191 (1986).

[8] C. Zhan, G. Sardina, E. Lushi, and L. Brandt, *Journal of Fluid Mechanics* **739**, 22 (2014).

[9] W. M. Durham, E. Climent, M. Barry, F. De Lillo, G. Boffetta, M. Cencini, and R. Stocker, *Nature Communications* **4**, 1 (2013).

[10] K. Gustavsson, F. Berglund, P. R. Jonsson, and B. Mehlig, *Physical Review Letters* **116**, 108104 (2016).

[11] M. Borgnino, G. Boffetta, F. De Lillo, and M. Cencini, *Journal of Fluid Mechanics* **856** (2018).

[12] S. O’Malley and M. Bees, *Bulletin of Mathematical Biology* **74**, 232 (2011).

[13] A. M. Roberts, *The Biological Bulletin* **210**, 78 (2006).

[14] S. Lovecchio, E. Climent, R. Stocker, and W. M. Durham, *Science Advances* **5**, 7879 (2019).

[15] W. M. Durham, J. O. Kessler, and R. Stocker, *Science* **323**, 1067 (2009).

[16] A. Sengupta, F. Carrara, and R. Stocker, *Nature* **543**, 555 (2017).

[17] F. De Lillo, M. Cencini, W. M. Durham, M. Barry, R. Stocker, E. Climent, and G. Boffetta, *Physical Review Letters* **112**, 044502 (2014).

- [18] M. Z. Sheikh, K. Gustavsson, D. Lopez, E. Lévéque, B. Mehlig, A. Pumir, and A. Naso, *Journal of Fluid Mechanics* **886**, A9 (2020).
- [19] K. Gustavsson, M. Z. Sheikh, D. Lopez, A. Naso, A. Pumir, and B. Mehlig, *New Journal of Physics* **21**, 083008 (2019).
- [20] V. Dabade, N. K. Marath, and G. Subramanian, *Journal of Fluid Mechanics* **778**, 133 (2015).
- [21] C. Siewert, R. Kunnen, M. Meinke, and W. Schröder, *Atmospheric research* **142**, 45 (2014).
- [22] K. Gustavsson, J. Jucha, A. Naso, E. Lévéque, A. Pumir, and B. Mehlig, *Physical Review Letters* **119**, 254501 (2017).
- [23] H. Brenner, *Journal of Fluid Mechanics* **11**, 604 (1961).
- [24] G. B. Jeffery, *Proceedings of the Royal Society of London. Series A* **102**, 161 (1922).
- [25] J. Qiu, Z. Cui, E. Climent, and L. Zhao, “Supplemental material: Fluid inertial torque is an effective gyrotactic mechanism for settling elongated micro-swimmers,” (2021).
- [26] S. Kim and S. J. Karrila, *Microhydrodynamics: principles and selected applications* (Butterworth-Heinemann, Boston, 1991).
- [27] T. J. Pedley and J. Kessler, *Proceedings of the Royal Society of London. Series B. Biological Sciences* **231**, 47 (1987).
- [28] T. J. Smayda, *Progress in Oceanography* **85**, 71 (2010).
- [29] J. Titelman and T. Kiørboe, *Marine Ecology Progress Series* **247**, 123 (2003).
- [30] D. Kamykowski, R. E. Reed, and G. J. Kirkpatrick, *Marine Biology* **113**, 319 (1992).
- [31] D. Lopez and E. Guazzelli, *Physical Review Fluids* **2**, 024306 (2017).
- [32] R. Monchaux, M. Bourgoin, and A. Cartellier, *Physics of Fluids* **22**, 103304 (2010).
- [33] M. N. Ardekani, G. Sardina, L. Brandt, L. Karp-Boss, R. N. Bearon, and E. A. Variano, *Journal of Fluid Mechanics* **831**, 655 (2017).
- [34] M. C. Davey and A. E. Walsby, *British Phycological Journal* **20**, 243 (1985).